International Journal of Engineering Research and Development
e-ISSN: 2278-067X, p-ISSN: 2278-800X, www.ijerd.com
Volume 10, Issue 8 (August 2014), PP.01-11

Evaluation of Noise Coefficients for Separate Gate InAlAs/InGaAs Double Heterostructure DG-HEMT

Parveen[1], Monika Bhattacharya[2], Jyotika Jogi[3]
[1,2,3]*Micro-Electronics Research Laboratory, Department of Electronic Science, A.R.S.D. College, University of Delhi, South Campus, New Delhi 110021, India*

Abstract:- This paper presents an analytical model for the evaluation of noise coefficients for separate Gate $In_{0.52}Al_{0.48}As/In_{0.53}Ga_{0.47}As$ DG-HEMT. The intrinsic noise sources due to voltage applied to the two gates are computed individually and the resultant noise coefficients are also evaluated. The analytical results show good agreement with the simulated data.

Keywords:- Double gate, HEMT, Noise coefficient, Separate gate, Silvaco Atlas Device simulator**.**

I. INTRODUCTION

InP based InAlAs/InGaAs High Electron Mobility Transistors have exhibited excellent performance with a high cut-off frequency exceeding 500 GHz for 25 nm gate-length single-gate device [1]. In terms of the noise performance, a low Minimum Noise Figure of 1.2 dB has also been achieved for 0.1 μm gate-length device at 94 GHz [2]. Such state-of-the art noise performance at ultra-high frequencies has made InP substrate based InAlAs/InGaAs HEMT the most promising candidate for future low-noise millimeter-wave frequency applications [1, 3]. Continuous shrinking of the gate length has been taking place over the past few decades to achieve higher cut-off frequency and better high speed performance and has now reached a limit beyond which the inevitable short-channel effects become dominant and cause degradation in the device performance. Further improvement in the device performance beyond the fundamental limit of device miniaturization calls for alternative solutions beyond gate-length shrinking. One such solution is modification in the conventional HEMT structure and employment of a double-gate structure (in which two gate are placed on each side of the conducting channel). 100 nm gate-length InAlAs/InGaAs double gate High Electron Mobility Transistor fabricated by *Vasallo et. al* have exhibited superior microwave and noise performance as compared to its single-gate counterpart [4-5] .With a purpose to explore the potential of this highly promising device, authors in their previous work presented a detailed analysis for the microwave performance assessment of InAlAs/InGaAs separate-gate DG-HEMT in terms of cut-off frequency (f_t) and maximum transducer power gain (G_u) [6-7].

In this paper, the earlier proposed charge control model is extended for a comprehensive noise performance analysis of InAlAs/InGaAs DG-HEMT operated in separate gate geometry. Various intrinsic noise sources, namely, drain noise current and gate noise current, are evaluated for separate gate DG-HEMT. In terms of these noise sources, the various noise coefficients, namely the drain noise coefficient (P), gate noise coefficient(R), and correlation coefficient(C) are obtained. The analytical results obtained are compared and is good agreement with Atlas Device simulation results. The operation of DG-HEMT in separate gate geometry offers a possibility of its application in mixers (where the radio frequency and the local oscillator frequency can be separately applied and controlled) and in velocity modulated transistors [8-11].

II. MODEL FORMULATION

A symmetric DG-HEMT with separate gate geometry is shown in Figure 1 The sheet carrier concentration (n_{si}) for either of the two 2DEGs in such a double-gate and double-heterostructure system is given by [12]:

$$n_{si} = \frac{\varepsilon}{qd}\left[V_{gsi} - V_{th} - E_{Fi}\right] \quad (1)$$

where, V_{gsi} represents the voltage at the two gates ($i = 1$ for gate1 and $i=2$ for gate2), q ($=1.6\text{x}10^{-19}\ C$) is the electron charge, ε ($= 12.03\varepsilon_o$) is the permittivity of $In_{0.53}Ga_{0.47}As$, ε_o ($= 8.85\text{x}10^{-12}\ F/m$) is the permittivity of free space, $d=d_d+d_i$ is the total thickness of InAlAs layer and $d_d=d_s+d_a$, where d_s ,d_a and d_i represent the thickness of the schottky layer, donor layer and spacer layer of the device respectively**.**

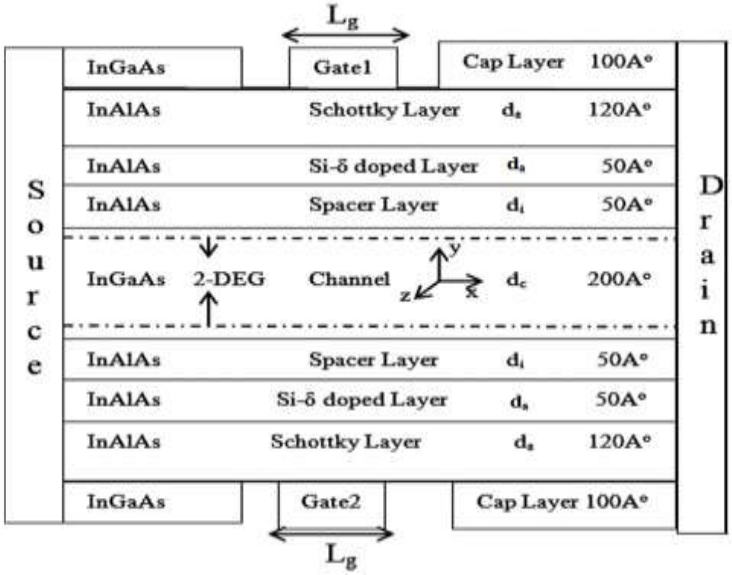

Fig.1: Double-gate InAlAs/InGaAs structure HEMT

The variation of fermi-level with the sheet carrier concentration n_{si} is incorporated as [12]:

$$E_{Fi} = k_1 + k_2\sqrt{n_{si}} + k_3 n_{si} \tag{2}$$

where k_1 *(0.143 V),* k_2 *(2.609* x 10^{-7} *Vcm*) and k_3 (*-5.469* x 10^{-14} *Vcm*^{2}) are the temperature dependent constants whose values are computed as illustrated in [12]. By substituting the expression for fermi potential from (2) in (1), the sheet carrier concentration (n_{si}) is obtained as

$$n_{si}(x) = \frac{\left(\sqrt{w_{1i}} - k_2^2\right)}{4k_4^2} \tag{3}$$

where $w_{1i} = k_2^2 + 4k_4\left|V_{off}\right|w_i$, $k_4 = k_3 + \frac{qd}{\varepsilon}$, $w_i = \frac{V_{gsi} - V_{off} - V(x)}{\left|V_{off}\right|}$ (4)

$$V_{off} = \Phi_b - \Delta E_c - \frac{qN_d d_d^2}{2\varepsilon_d} + k_1 \tag{5}$$

where *V(x)* is the channel potential at any point *x*. L_1 is the point in the channel where electrons reach their saturation velocity, Φ_b *(=0.56eV)* is the schottky barrier height, ΔE_c *(=0.52eV)* is the conduction band discontinuity and ε_d *(*=12.47ε_o*)* permittivity of $In_{0.53}Al_{0.47}As$ [13].

Using (3), and linear piecewise velocity field relation, total current flowing through the channel due to both the 2DEGs is evaluated as follows:

$$I_{ds} = \sum_{i=1}^{2} I_{dsi} \tag{6}$$

where I_{dsi} represents component of current due to voltage applied at gate1 (when i=1) and current due to voltage applied at gate2 (when i=2)

$$I_{dsi} = \begin{cases} \frac{qZ\mu}{8k_4^2}\left[\left(\frac{s_{1i}^2 - p_{1i}^2}{4}\right) - 2k_2\left(\frac{s_{1i}^{3/2} - p_{1i}^{3/2}}{3}\right) + k_2^2\left(\frac{s_{1i} - p_{1i}}{4}\right)\right]; & x \le L_1 \quad (Linear \ \text{Re}\, gion) \\ \frac{qZV_{sat}}{4k_4^2}\left(\sqrt{p_{1i}} - k_2\right)^2; & x > L_1 \quad (Saturation \ \text{Re}\, gion) \end{cases} \tag{7}$$

$s_{1i} = w_{1i}(x=0)$, $p_{1i} = w_{1i}(x=L_1)$, Z *(=100 μm)* is gate width, μ *(=0.83 m*^{2}*/V-sec)* is electron mobility, V_{sat} (= *2.63*x10^5 *m/sec*) is the saturation velocity [13]. L_1 is the linear region length and is obtained using (7) as [14]

$$L_1 = \frac{1}{2k_4 E_c\left(\sqrt{p_{1i}} - k_2\right)^2}\left[\left(\frac{{s_{1i}}^2 - {p_{1i}}^2}{4}\right) + \left(\frac{2k_2\left({s_{1i}}^{3/2} - {p_{1i}}^{3/2}\right)}{3}\right) + \left(\frac{{k_2}^2\left(s_{1i} - p_{1i}\right)}{2}\right)\right] \tag{8}$$

where $E_c = \frac{V_{sat}}{\mu}$ is the critical filed.

A. DRAIN NOISE COEFFICIENT (P)

Johnson noise source produced across an infinitesimally small segment $x_o<x<x_o+\Delta x$ in the linear region is evaluated as [15]:

$$\overline{\Delta V_{xoi}^2} = 4kT_{ei}\Delta f\left(\frac{dV(x)}{I_{dsi}}\right) \tag{9}$$

where Δf is the bandwidth and $dV(x)/I_{dsi}$ represent the incremental channel resistance. The effective noise temperature (T_{ei}) is given by [16]:

$$T_{ei} = T_o\left(1 + \delta\left(\frac{p_i^3}{w_i^3}\right)\right) \tag{10}$$

where T_o(=*300 K*) is the ambient temperature and δ is the noise temperature constant which is related to the field dependence of electron temperature in the channel [15].

Each elementary thermal noise source generated across a small segment $x_o<x<x_o+dx$ in the linear region leads to voltage fluctuation across the drain to source terminal and is given by [17]:

$$\overline{\Delta v_{d1i}} = \left(\frac{w_i}{p_i}\right)\Delta V_{xoi}\cosh\left(\frac{\pi L_2}{2d}\right) \tag{11}$$

Integrating (11) across the entire linear region, the net open circuit voltage fluctuation due to Johnson noise is evaluated as [13]:

$$\left|\overline{\Delta v_{d1i}^2}\right| = \frac{16kT_0\Delta f\, k_4^2\left|V_{off}\right|}{qZV_{sat}\left(\sqrt{p_{1i}} - k_2\right)^2}\cosh^2\left(\frac{\pi L_2}{2d}\right)\left(\frac{1}{p_i^2}\left(\frac{s_i^3 - p_i^3}{3}\right) + \delta\, p\ln\left(\frac{s_i}{p_i}\right)\right) \tag{12}$$

Noise generated in saturation region also known as the diffusion noise, is interpreted as being caused due spontaneous generation of dipole layers which drift with the saturation velocity V_{sat} and is expressed as [15-17]:

$$\overline{\Delta v_{d2i}^2} = \frac{64\,q\,D\,\Delta f\, I_{dsi}(d+b_i)^3}{\pi^5 V_{sat}^3 \varepsilon^2 {b_i}^2 Z^2}\sin^2\left(\frac{\pi b_i}{2(d+b_i)}\right)\left(3 + \exp\left(\frac{\pi L_2}{(d+b_i)}\right) - 4\exp\left(\frac{\pi L_2}{(d+b_i)}\right) + \frac{\pi L_2}{(d+b_i)}\right) \tag{13}$$

where D is the diffusion noise coefficient. It is related to the diffusion of carriers in high field condition with value ranging from 35cm^2/s to 55 cm^2/s [15], $L_2=L_g-L_1$ is the saturation region length, b_i is the effective channel thickness and is evaluated as [18]

$$b_i = \frac{\varepsilon}{q}\left(\frac{k_2 k_4}{\left(\sqrt{p_{1i}} - k_2\right)} + k_3\right) \tag{14}$$

The net drain noise current due to the voltage applied at both the gates is then expressed as:

$I_d = \sum_{i=1}^{2} I_{di}$ where $\overline{I_{di}^2} = \frac{\left|\overline{v_{d1i}^2}\right| + \left|\overline{v_{d2i}^2}\right|}{R_{di}}$,

R_{di} is the drain to source resistance defined as ratio of the differential change in drain voltage to the differential change in drain to source current producing it when the gate voltage is fixed, and is obtained using (7) as

$$R_{di} = \left.\frac{dV_{ds}}{dI_{dsi}}\right|_{V_{gsi=constant}} \tag{15}$$

Drain noise coefficient (P) is directly related to the mean square drain noise current and inversely proportional to the transconductance. Mathematically, it is evaluated as:

$$P = \frac{\overline{I_D^2}}{4kT_0\,\Delta f\,G_{mT}}$$

where G_{mT} is the total transconductance is evaluated using (6) as

$$G_{mT} = \sum_{i=1}^{2} G_{mi} \quad \text{where } G_{mi} = \left.\frac{dI_{ds}}{dV_{gsi}}\right|_{V_{ds=constant}} \tag{16}$$

A lower value of drain noise current and higher transconductance is desirable for a lower value of drain noise coefficient P which is an indicator of better noise performance.

B. GATE NOISE COEFFICIENT (R)

The gate noise current due to elementary Johnson noise produced in the linear region of the channel is given by

$$\Delta i_{g1i} = j\omega\Delta q_{1i} \tag{17}$$

where, Δq_{1i} is the induced gate charge that is produced by an elementary thermal noise voltage and is expressed as [17-19]

$$\Delta q_{1i} = -\frac{qZ\left|\overline{\Delta v_{d1i}^2}\right|L_1}{2k_4^2 R_{di} I_{d1i}}\left(\kappa_1^{'} - \gamma_i\beta_i\right) \tag{18}$$

Integrating over the entire region length, the mean square gate noise current due to thermal noise is obtained as:

$$\overline{i_{g1i}^2} = \frac{64kT_o\Delta f\,\omega^2 L_1^2\left|V_{off}\right|k_4^2}{qZR_{di}^2 V_{sat}^3\left(\sqrt{p_{1i}} - k_2\right)^6}\cosh^2\left(\frac{\pi L_2}{2d}\right)\left(R_{0i} + R_{1i} + R_{2i} + R_{3i}\right) \tag{19}$$

where

$$R_{0i} = \frac{1}{p_i^2}\left[X_i^2\left(\frac{\left(s_i^3 - p_i^3\right)}{3}\right) + 2\gamma_i QX_i\left(\frac{\left(s_i^4 - p_i^4\right)}{4}\right) + \gamma^2\left(Q^2\left(\frac{\left(s_i^5 - p_i^5\right)}{5}\right) + Qk_2^2\left(\frac{\left(s_i^4 - p_i^4\right)}{2}\right) + k_2^4\left(\frac{\left(s_i^3 - p_i^3\right)}{3}\right)\right)\right] \tag{20}$$

$$R_{1i} = \frac{1}{p_i^2}\frac{4k_2}{105Q^3}\left\{\gamma_i X_i\left(\left(-k_2^4\left(s_{1i}^{3/2} - p_{1i}^{3/2}\right) + 3k_2^2 Q\left(s_i s_{1i}^{3/2} - p_i p_{1i}^{3/2}\right) - \frac{15}{2}Q^2\left(s_i^2 s_{1i}^{3/2} - p_i^2 p_{1i}^{3/2}\right)\right) + \gamma_i^2\left(\left(k_2^6\left(\frac{\left(s_{1i}^{3/2} - p_{1i}^{3/2}\right)}{3}\right)\right.\right.\right.$$

$$\left.\left.\left. - k_2^4 Q\left(s_i s_{1i}^{3/2} - p_i p_{1i}^{3/2}\right) + \frac{15}{3}Q^2 k_2^2\left(\frac{s_i^2 s_{1i}^{3/2} - p_i^2 p_{1i}^{3/2}}{2}\right) - \frac{35}{2}Q^3\left(\frac{s_i^3 s_{1i}^{3/2} - p_i^3 p_{1i}^{3/2}}{3}\right)\right)\right)\right\} \tag{21}$$

$$R_{2i} = \delta p_i\left(X_i^2\ln\left(\frac{s_i}{p_i}\right) + 2\gamma_i QX_i\left(s_i - p_i\right) + \gamma_i^2\left(Q^2\left(\frac{\left(s_i^2 - p_i^2\right)}{2}\right) + 2k_2^2 Q\left(s_i - p_i\right) + k_2^4\ln\left(\frac{s_i}{p_i}\right)\right)\right) \tag{22}$$

$$R_{3i}=\delta p_i\,2k_2\left(\left(\left(2\gamma_i X_i\left(k_2\left(\tanh^{-1}\left(\frac{\sqrt{s_{1i}}}{k_2}\right)-\tanh^{-1}\left(\frac{\sqrt{p_{1i}}}{k_2}\right)\right)-\left(\sqrt{s_{1i}}-\sqrt{p_{1i}}\right)\right)-\frac{\gamma^2}{3}\left(s_{1i}^{3/2}-p_{1i}^{3/2}\right)\right)\right)\right) \tag{23}$$

where

$$\gamma_i=\frac{q\,Z\,\mu\,p_i\left|V_{off}\right|R_{di}}{k_4\cosh\left(\frac{\pi L_2}{2d}\right)L_1},\ \kappa_i^{'}=\kappa_i+\frac{L_2}{L_1}\left(\sqrt{p_{1i}}-k_2\right)^2 \tag{24}$$

$$\kappa_i=\frac{1}{2k_4E_c\left(\sqrt{p_{1i}}-k_2\right)^2L_1}\left[\frac{1}{4}\left(\frac{s_{1i}^3-p_{1i}^3}{3}\right)-\frac{11}{6}k_2\left(\frac{s_{1i}^{5/2}-p_{1i}^{5/2}}{5/2}\right)+\frac{7}{6}k_2^2\left(\frac{s_{1i}^2-p_{1i}^2}{6}\right)-k_2^3\left(\frac{s_{1i}^{3/2}-p_{1i}^{3/2}}{3}\right)-f'(s_{1i})(s_{1i}-p_{1i})+2k_2f'(s_{1i})\left(\sqrt{s_{1i}}-\sqrt{p_{1i}}\right)\right] \tag{25}$$

$$f'(s_{1i})=\frac{s_{1i}^2}{4}-2k_2\frac{s_{1i}^{3/2}}{3}+\frac{k_2^2}{2}s_{1i},\ \beta_i=2k_2\left(\sqrt{w_{1i}}-\sqrt{p_{1i}}\right)-\left(w_{1i}-p_{1i}\right) \tag{26}$$

$$X_i=\kappa_i^{'}-\gamma_i\left(p_{1i}-2k_2\sqrt{p_{1i}}\right),\ Q=2k_4\left|V_{off}\right| \tag{27}$$

Similarly, the gate noise current due to diffusion noise in the saturation region is evaluated by substituting γ_i =0 in (18) and is expressed as:

$$\overline{i_{g2i}^2}=\frac{16q^3\omega^2D\Delta f(d+b_i)^3L_1^2\kappa_i^{'2}}{\pi^5R_{di}^2V_{sat}^3\varepsilon^2b_i^2k_4^4I_{dsi}}\sinh^2\left(\frac{\pi b_i}{2(d+b_i)}\right)\left[3+\left(\frac{\pi\ L_2}{(d+b_i)}\right)+\exp\left(\frac{\pi\ L_2}{(d+b_i)}\right)-4\exp\left(\frac{\pi\ L_2}{2(d+b_i)}\right)\right] \tag{28}$$

Gate Noise Coefficient (R) is directly related to the mean square gate noise current and inversely proportional to the square of gate to source capacitance and is expressed as:

$$R=\sum_{i=1}^{2}R_i\ ,\ \text{where}\ R_i=\frac{\overline{i_{g1i}^2}+\overline{i_{g2i}^2}}{4kT_0\,\Delta f\,\omega^2{C_{gsi}}^2}G_{mi} \tag{29}$$

C_{gsi} is the gate to source capacitance and is expressed using (3) as [17]

$$C_{gsi}=\left.\frac{dQ_{1i}}{dV_{gsi}}\right|_{Vds}+\left.\frac{dQ_{2i}}{dV_{gsi}}\right|_{Vds} \tag{30}$$

where, total charge in region-I is given by $Q_{1i}=\int_0^{L_1}qZn_{si}(x)\,dx$ and total charge in region-II is given by $Q_{2i}=qZn_{si}(L_1)L_2$

This implies that a lower gate noise current along with a higher gate to source capacitance is desirable for lower R. On the other hand, a lower gate to source capacitance is required for higher cutoff frequency. Double-gate HEMT in separate gate geometry provides an additional control for optimization of device performance for ensuring good noise behaviour as well as high cut-off frequency.

C. CORRELATION COEFFICIENT (C)

Any fluctuation in the current flowing through the channel contributes to both drain noise current as well as the gate noise current, therefore, they are correlated. The correlation between Johnson noise induced drain noise current and gate noise current in linear region is obtained by using (12) and (19) as: [15,17]

$$\overline{i_{g1i}{}^{*}i_{d1i}}=\frac{j\omega2k\,T_o\,\Delta f\,q\,Z\left|V_{off}\right|L_1}{k_4^2I_{di}^2R_{di}^2}\cosh^2\left(\frac{\pi L_2}{2d}\right)\left(S_{oi}+S_{1i}+S_{2i}+S_{3i}\right) \tag{31}$$

where

$$S_{oi} = -\frac{1}{p_i^2}\left[X_i \left(\frac{s_i^3 - p_i^3}{3} \right) + \gamma_i \left(k_2^2 \left(\frac{s_i^3 - p^3_i}{3} \right) \right) + Q \left(\frac{s_i^4 - p^4_i}{4} \right) \right] \tag{32}$$

$$S_{1i} = \frac{2\gamma_i k_2}{p_i^2 Q^3}\left[\left(\left(\frac{s_i^{7/2} - p_i^{7/2}}{7/2} \right) - 2k_2^2 \left(\frac{s_i^{5/2} - p_i^{5/2}}{5/2} \right) + k_2^4 \left(\frac{s_i^{3/2} - p_i^{3/2}}{3/2} \right) \right) \right] \tag{33}$$

$$S_{2i} = -\delta p_i \left[X_i \log\left(\frac{s_i}{p_i} \right) + \gamma_i \left(k_2^2 \left(\frac{s_i}{p_i} \right) + Q(s_i - p_i) \right) \right] \tag{34}$$

$$S_{3i} = 4\delta p_i k_2 \gamma_i \left[\left(\sqrt{s_{1i}} - \sqrt{p_{1i}} \right) + k_2 \tanh\left(\frac{\sqrt{p_{1i}} - \sqrt{s_{1i}}}{k_2} \right) \right] \tag{35}$$

and therefore, the correlation coefficient between drain noise current and gate noise current in linear and saturation region is expressed as:

$$C_{1i} = C_{11i}\left(\frac{P_{1i} R_{1i}}{P_i R_i} \right)^{1/2} + C_{22i}\left(\frac{P_{2i} R_{2i}}{P_i R_i} \right)^{1/2} \tag{36}$$

where

$$C_{11i} = \frac{\overline{i_{g1i} * i_{d1i}}}{j\sqrt{\overline{i^2_{g1i}} * \overline{i^2_{d1i}}}} \text{ and } C_{22i} = \frac{\overline{i_{g2i} * i_{d2i}}}{j\sqrt{\overline{i^2_{g2i}} * \overline{i^2_{d2i}}}} = 1 \tag{37}$$

Due to capacitive coupling between the gate and the drain, the diffusion noise induced drain noise current I_{d2i} and gate noise current I_{g2i} are fully correlated. Therefore C_{22i}=1

III. RESULT AND DISCUSSION

The variation of mean square drain noise current and mean square gate noise current with gate1 voltage (V_{gs1}) , when gate2 voltage is kept fixed at V_{gs2}= -0.3 V is shown in Figure 2. For low values of V_{gs2}, the sheet

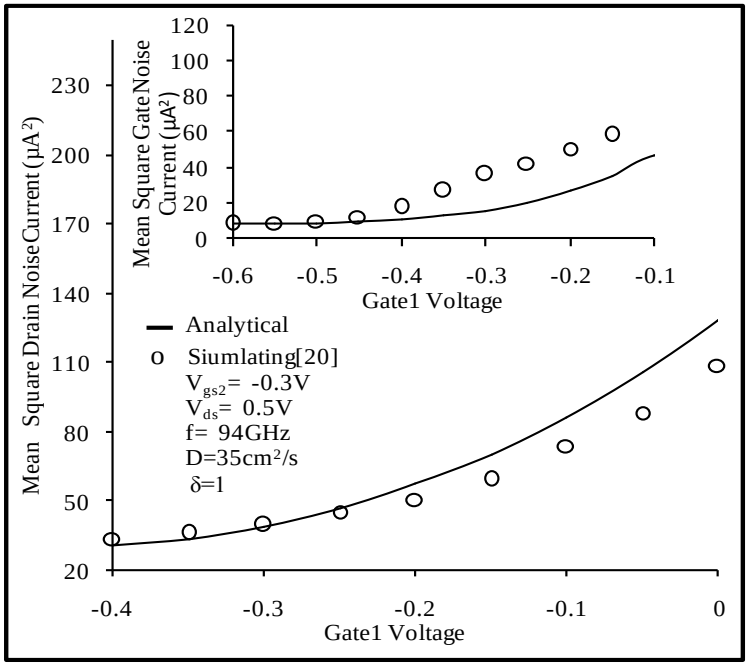

Fig.2: Variation of mean square drain noise current with gate1 voltage (V_{gs1}), (inset) Variation of mean square gate noise current with gate1 voltage (V_{gs1})

carrier concentration is low and hence the corresponding fluctuation in the current flowing through the channel is low. As a result, the intrinsic noise current sources, namely the gate noise current and the drain noise current are also low. For higher values of V_{gs2}, the current flowing through the channel increases. This leads to a greater charge fluctuation which in turn results in a higher value of gate noise current and drain noise current. As also shown in the figure, in a DG-HEMT operated in separate gate-geometry, the current flowing through the channel and hence the intrinsic noise sources (gate noise current and drain noise current) can be controlled by varying voltage at either of the two gates keeping the voltage at the other gate fixed. The analytical results obtained are also compared and found to be in good agreement with the results obtained using the 'Electron Noise Simulator Module' of ATLAS device simulation software [20]

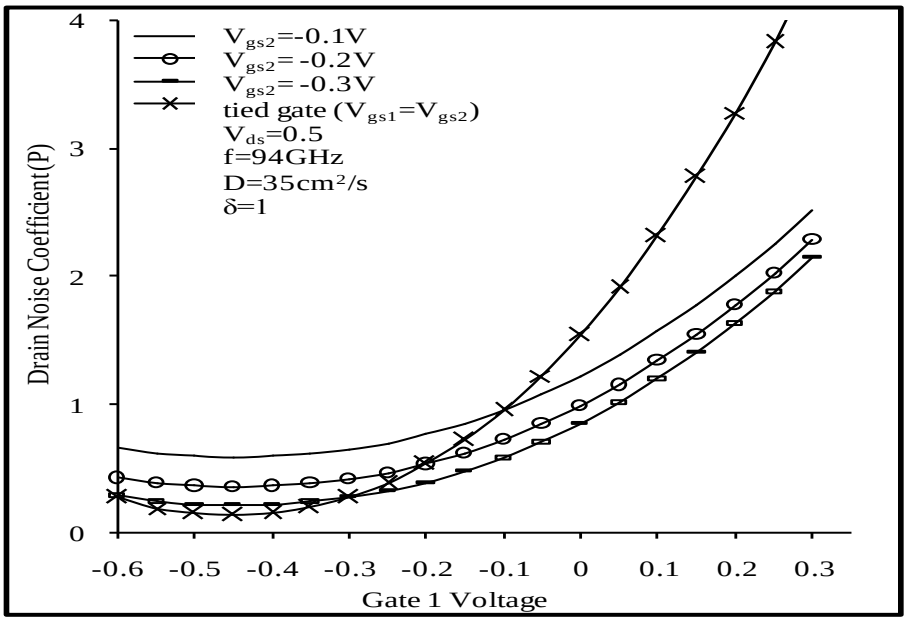

Fig. 3: Variation of Drain Noise Coefficient with gate1 voltage for different values of gate2 voltage (V_{gs2})

Figure 3 shows the variation of drain noise coefficient (P) with gate1 voltage (V_{gs1}) for different values of gate2 voltage (V_{gs2}). As shown in the figure, intially for low value of V_{gs1} (< -0.3V) when drain noise current is low, P decreases with increase in V_{gs1}. This occurs due to increase in transconductance (g_m) with the increase in V_{gs1}. But for higher values of V_{gs1} (>-0.3V), the diffusion noise induced drain noise current increases and becomes dominant. As a result, the drain noise coefficient (P) increases with increase in $V_{gs1.}$ Similarly, increase in voltage applied at gate2 (V_{gs2}) also leads to increase in P. As shown in the figure, when the voltage applied at gate2 is increased from -0.3 V to -0.1 V, P increases from 0.849 to 1.22 at V_{gs1}=0V. The variation of drain noise coefficient with gate1 voltage (V_{gs1}) for a fixed gate2 voltage (V_{gs2}) in a separate-gate geometry DG-HEMT is also compared with that of tied-gate geometry DG-HEMT (V_{gs1}=V_{gs2}). As shown in figure, in a tied-gate geometry DG-HEMT, the variation of drain noise coefficient with the voltage applied at the two gates is fixed. However, in a separate gate geometry DG-HEMT, the slope of the variation of P with gate voltage and hence the overall noise behaviour of the device can be better controlled by varying the voltage applied at either of the two gates and keeping the voltage at the other gate fixed.

Figure 4 shows the variation of drain noise coefficient (P) with gate2 voltage (V_{gs2}) at V_{gs1}= -0.1 V for different values of diffusion noise coefficient (D). As shown in the figure, when the diffusion coefficient D is increased from 35cm^2/s to 55cm^2/s at V_{gs2}= 0V, P increases from 1.27 to 1.98. This occurs due to increase in diffusion noise induced drain noise current with increase in D. The variation of P, with gate1 voltage (V_{gs1}) for different values of noise temperature constant (δ) is also shown in Figure 4(inset). The increase in the noise temperature constant δ causes increase in the Johnson noise induced drain noise current. As the value of δ increases from δ=1 to δ=3 at V_{gs1}= -0.3V, P increases from 0.975 to 1.023.

As also evident from the figure, while the effect of diffusion noise coefficient is most prominent at higher values gate1 voltage where the diffusion noise dominates, the effect of noise temperature constant on the other hand is observed to be most siginificant at lower values of gate1 voltage where the Johnson noise is dominant.

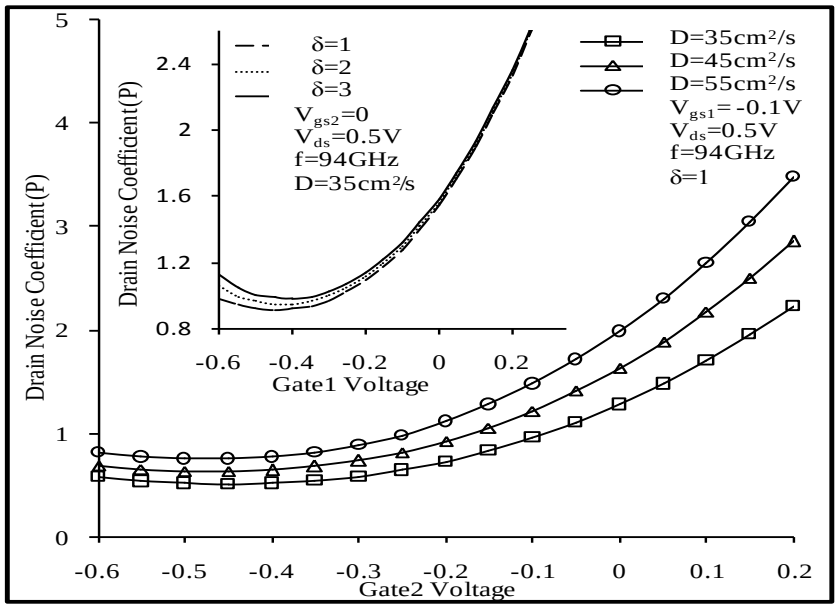

Fig.4: Drain noise coefficient with gate2 voltage,at different values of diffusion noise coefficient (D) (inset)Drain noise coefficient with gate1 voltage,at different values of noise temperature constant (δ)

Figure 5 shows the variation of gate noise coefficient (R) with gate1 voltage (V_{gs1}) for the different values of gate2 voltage (V_{gs2}). As shown in the figure, the gate noise coefficient (R) initially decreases very sharply with increase in V_{gs1} due to increase in the gate to source capacitance (C_{gs}). For higher values of V_{gs1}, when the diffusion noise induced gate noise current increases and begins to dominate, R decreases at a much slower rate and eventually begins to increase with increase in V_{gs1}. The increase in voltage applied at gate2 (V_{gs2}) also has a similar effect on the R. As voltage applied at gate2 is increased from -0.2 V to 0 V, the gate noise coefficient (R) increases from 3.56 to 8.66 at V_{gs1} = -0.3 V. The variation of Correlation coefficient (C) with gate2 voltage (V_{gs2}) for the different value of gate1 voltage (V_{gs1}) is shown in Figure 5(inset) when D=35cm^2/s, f=94GHz and δ=1. The correlation coefficient (C) is observed to increase with increase in gate2 voltage which occurs due to higher correlation between the Johnson noise induced drain noise current and gate noise current.

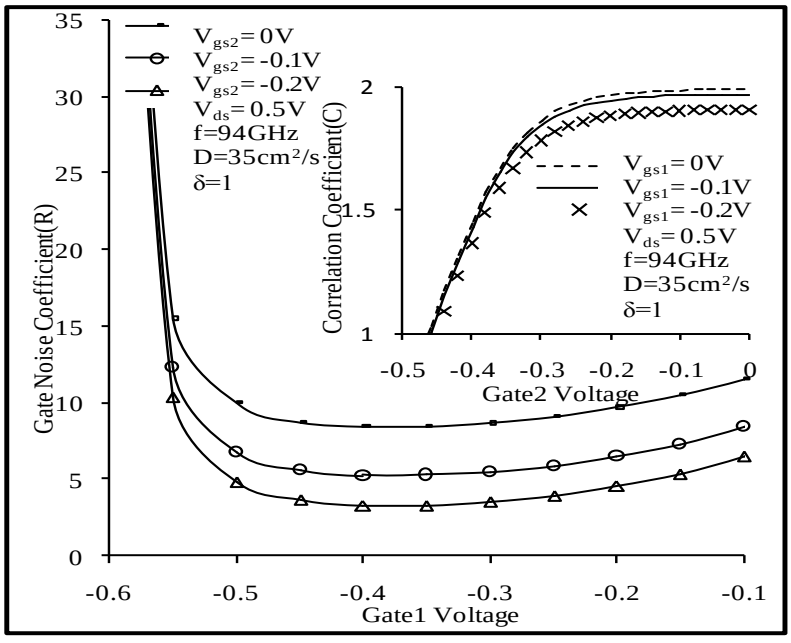

Fig. 5: Variation of gate noise coefficient with gate1 voltage (V_{gs1}) for different values of gate2 voltage, (inset) Correlation Coefficient (C) with gate2 voltage for different values of gate1 voltage

Also, when V_{gs1} is increased from -0.2V to 0V, C increases from 1.904 to 1.99 at V_{gs2}= -0.1V. This occurs due to increase in the diffusion noise induced gate noise current. In a separate gate geometry DG-HEMT,

the noise coefficients R and C can be varied by varying the voltage applied at any of the two gates keeping the voltage applied at the other gate constant.

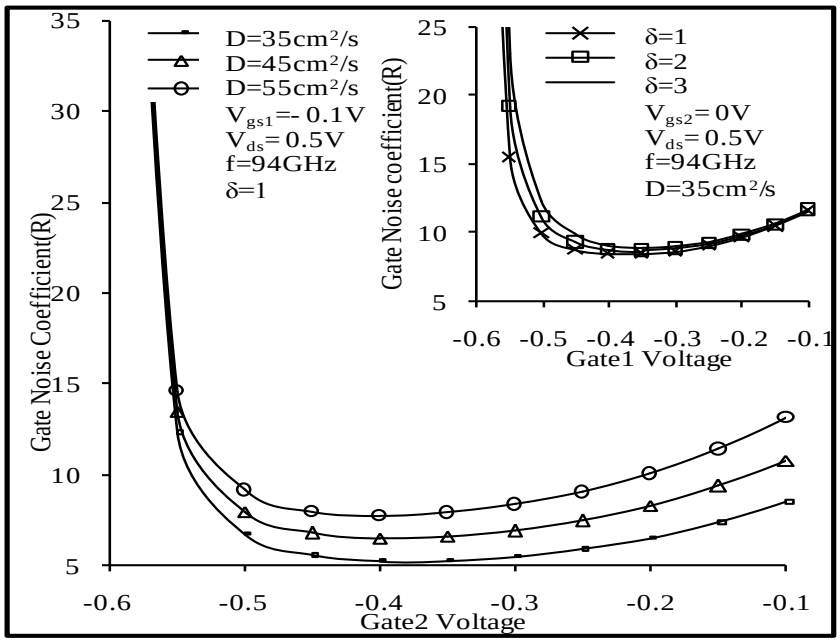

Fig. 6: Variation of gate noise coefficient with gate2 voltage,at different value of D (inset) variation of gate noise coefficient with gate1 voltage, at different value of δ

Figure 6 shows the variation of gate noise coefficient (R) with gate2 voltage (V_{gs2}) for the different values of diffusion noise coefficient (D) when δ=1. As shown in the figure, the gate noise coefficient R increases with diffusion noise coefficient and the impact of Diffusion Coefficient D on the gate noise coefficient is most significant at higher values of gate2 voltage where diffusion noise is dominant. Figure 6(inset) illustrates the effect of noise temperature constant (δ) on the gate noise coefficient R. As shown in the figure, the noise temperature constant influences the gate noise current and hence the gate noise coefficient R over the entire range of gate1 voltage V_{gs1}. However, its impact is more prominent at low values of V_{gs1}, where thermal noise is dominant.

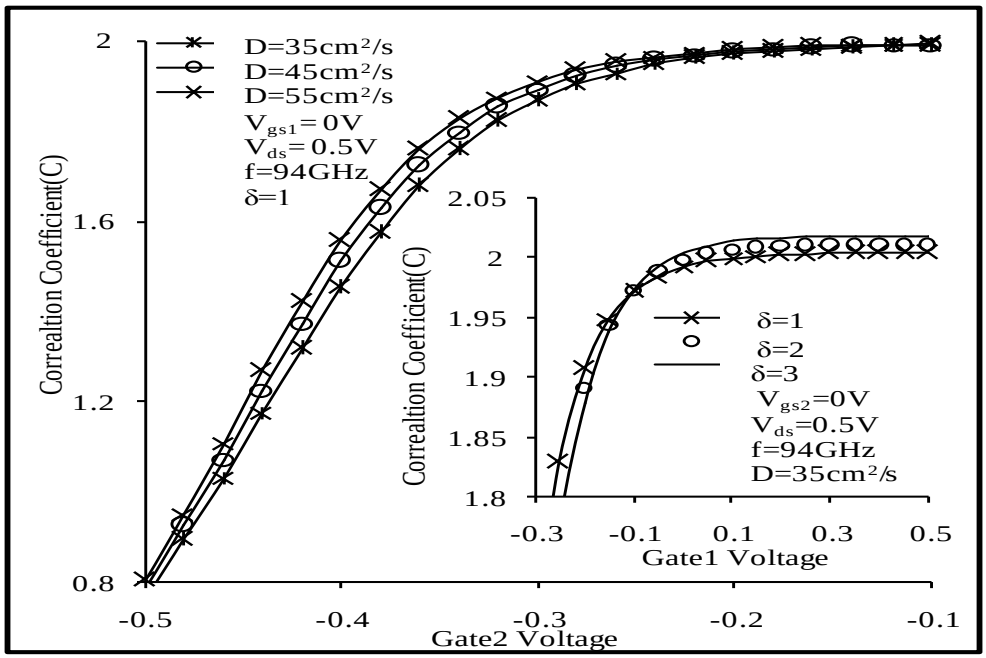

Fig.7: Correlation coefficient with gate2 voltage,at different value of diffusion noise constant (D), (inset) Correlation coefficient with gate1 voltage,at different value of noise temperature constant.(δ)

Figure 7 shows the variation of Correlation coefficient (C) with gate2 voltage (V_{gs2}) for different values of diffusion noise coefficient (D). As shown in the figure, as the value of D is varied from 35cm^2/s to 55 cm^2/s, the value of C increases from 1.67 to 1.751 at V_{gs2}= -0.35 V. This occurs due increase in the drain noise and gate noise current which cause increase in the value of drain noise and gate noise coefficient with increase in D. The variation of Correlation coefficient (C) with gate1 voltage (V_{gs1}) for different values of δ, is also shown in Figure 7(inset). As the noise temperature constant is increased from δ=1 to δ=3, the correlation coefficient (C), increases from 1.9 to 2.04 at V_{gs1}= 0V. Therefore, both δ and D have a significant influence on correlation coefficient over the entire range of gate voltage.

IV. CONCLUSION

A charge control based analytical model is presented for studying the noise performance of separate-gate geometry InAlAs/InGaAs DG-HEMT. Analytical expressions for the intrinsic noise sources, namely, the gate noise current and the drain noise current, are derived. The noise performance assessment is then performed in terms of the various noise coefficients including drain noise coefficient, gate noise coefficient and correlation coefficient. The effect of voltage applied individually at the two gates, on the noise performance of the device is studied. It has been observed that in a separate gate-geometry double-gate HEMT, the noise coefficients and hence the overall noise behaviour of the device can be controlled by varying the voltage applied at any of the two gates with the voltage at the other gate kept constant. This is a very useful feature of a double-gate HEMT operated in separate gate geometry which can be employed for its usage in various applications such as in mixers. In addition to this, the effect of two major modeling parameters, namely, diffusion noise constant and noise temperature constant, on noise coefficients is also studied. The results obtained using the proposed analytical model are compared and found to be in good agreement with the results obtained using Atlas device Simulator. The analysis presented in the paper can be further extended for the evaluation of various major noise performance parameters like minimum noise figure and minimum noise temperature for separate gate DG-HEMT.

ACKNOWLEDEGMENT

The authors acknowledge, University Grant Commission (UGC) for providing the finical support for the work.

REFERENCES

[1]. Y.Yoshimi, A. Endoh, K.Shinohara, K.Hikosaka, T.Matsui, S. Hiyamizu, and T.Mimura, "Pseudomorphic $In_{0.52}Al_{0.48}As/In_{0.7}Ga_{0.3}As$ HEMTs with an ultrahigh f_T of 562 GHz," IEE Electron Device Letters, vol.23,no.10,pp.573-575,Oct. 2002.

[2]. K. H. G. Duh, P. C. Chao, S. M. J. Liu, P. Ho, M. Y.Kao, and J. M. Ballingall, "A super low-noise 0.1 μm T- gate InAlAs-InGaAs-InP HEMT, "IEEE Microwave and Guided Wave Letters,vol.1,no.5, pp.114-116,May 1991.

[3]. Suemitsu, Tetsuya, and Masami Tokumitsu,"InP HEMT technology for high-speed logic and communications," IEICE transactions on electronics, vol.E90-C ,no.5, pp.917-922, May 2007.

[4]. B.G.Vasallo, N.Wichmann, S.Bollaert, Y.Roelens, A.Cappy, T. Gonzalez, D.Pardo and J.Mateos, "Comparison Between the Dynamic Performance of Double- and Single-Gate AlInAs/InGaAs HEMTs," IEEE Trans Electron Device, vol.54,no.11,pp.2815-2822, Nov. 2007.

[5]. B. G. Vasallo, N.Wichmann, S.Bollaert, Y.Roelens, A.Cappy, T.Gonzalez, D.Pardo and J.Mateos, "Comparison Between the Noise Performance of Double- and Single-Gate AlInAs/InGaAs HEMTs," IEEE Trans Electron Device, vol.55, no.6, pp.1535-1540, June 2008.

[6]. Parveen, R.S. Gupta ,M. Gupta and J.Jogi, "Intrinsic Admittance, Parameter For Separate Gate InAlAs/InGaAs DG-HEMT For 100 nm Gate length," in Proc.of 2013 IEEE Conference on Information and Communication Technologies (ICT 2013),pp.750-754.

[7]. Parveen, M.Gupta, R.S Gupta and J.Jogi, "RF Characterization of 100 nm Separate Gate InAlAs/InGaAs DG-HEMT," Microwave Opt. Tech. Letter, vol.55no.11, pp.2796-2803, Nov. 2013.

[8]. C. Tsironis ,R. Meierer and R.Stahlman, "Dual gate MESFET Mixers," IEEE Trans Microwave Theory and Techniques vol.32,no.3,pp.248-255,March 1984.

[9]. A.J. Bergsma and B.A. Syrett , "A Comprehensive Design Method for Dual-Gate MOSFET Mixers," IEEE Trans circuit and systems-II: Analog and Digital signal processing, vol.47,no.12,pp.1443-1451, Dec. 2000.

[10]. B.G. Vasallo, N. Wichmann, S. Bollaert, Y. Roelens, A. Cappy, T. Gonzalez, D.Pardo and J.Mateos, "Monte Calro Study of the Dynamic Performance of a 100-nm- Gate InAlAs/InGaAs Velocity Modulated Transistor," IEEE Trans Electron Device, vol.57,no.10,pp.2572-2578, Oct. 2010.

[11]. C. Sampedro, F. Gamiz, A. Godoy ,M. Prunnila and J.Ahopelto, "A comprehensive study of carrier velocity modulation in DGSOI transistors," Solid State Electronics, vol. 49,pp.1504-1509,Sept. 2005.

[12]. N. Dasgupta , A. Dasgupta, "An analytical expression for sheet carrier concentration vs. gate voltage for HEMT modeling," Solid State Electronics, vol.36,no.2,pp.201-203,1993.

[13]. M.Bhattacharya, J. Jogi, R.S Gupta, M. Gupta, "Impact of Doping concentration and donor-layer thickness on the dc characterization

[14]. of symmetric double-gate and single-gate InAlAs/InGaAs/InP HEMT for nanometer gate dimension-A comparison," In: IEEE TENCON 2010 conference proceedings, November 21–24 (2010); Japan Fukuoka, pp.134–139

[15]. T.M. Brookes, "The Noise Properties of High Electron Mobility Transistors," IEEE Trans Electron Devices , vol.ED-33,no.1, pp.52-57, Jan.1986

[16]. R.A. Pucel, H.A. Haus and H. Staz,, "Signal and noise properties of GaAs microwave FET," Advanced in Electronics and Electron Physics, New York :Acadmic, pp.195-265, 1975

[17]. W. Baechtold, "Noise behavior of GaAs field effect transistor with short gate length," IEEE Trans. Electron Devices vol.ED-19, no.5, pp.674-680, May 1972

[18]. V. Guru, H.P. Vyas, M. Gupta and R.S. Gupta, "Analytical noise model of high electron mobility transistor for microwave frequency application," Microwave Opt. Tech. Letters. vol.40,no.5,pp.410-417, March 2004

[19]. M.J. Moloney , F.Ponse and H. Morkoc, "Gate Capacitance-Voltage Characteristic of MODFET's: Its Effect on Transconductance ," IEEE Trans. Electron Devices, vol.ED.32,no.9,pp.1675-1684,Sept.1985

[20]. H.Statz, H.A. Haus and R.A. Pucel , "Noise Characteristics of gallium arsenide filed effect transistor," IEEE Trans. Electron Device, vol.ED-21,no.9,pp.549-562, Sept. 1974

[21]. Silvaco Atlas Device simulator 2010